View metadata, citation and similar papers at core.ac.uk
brought to you by CORE
provided by Elsevier - Publisher Connector

# Distinct Roles for Secreted Semaphorin Signaling in Spinal Motor Axon Guidance

**Andrea B. Huber,[1,4] Artur Kania,[2,3] Tracy S. Tran,[1] Chenghua Gu,[1] Natalia De Marco Garcia,[3] Ivo Lieberam,[3] Dontais Johnson,[1] Thomas M. Jessell,[3] David D. Ginty,[1,*] and Alex L. Kolodkin[1,*]**

[1] Howard Hughes Medical Institute
Department of Neuroscience
The Johns Hopkins University School of Medicine
Baltimore, Maryland 21205

[2] Neural Circuit Development Laboratory
Institut de Recherches Cliniques de Montréal
Montréal, Quebec H2W 1R7
Canada

[3] Howard Hughes Medical Institute
Department of Biochemistry and Molecular Biophysics
Center for Neurobiology and Behavior
Columbia University
New York, New York 10032

## Summary

**Neuropilins, secreted semaphorin coreceptors, are expressed in discrete populations of spinal motor neurons, suggesting they provide critical guidance information for the establishment of functional motor circuitry. We show here that motor axon growth and guidance are impaired in the absence of Sema3A-Npn-1 signaling. Motor axons enter the limb precociously, showing that Sema3A controls the timing of motor axon in-growth to the limb. Lateral motor column (LMC) motor axons within spinal nerves are defasciculated as they grow toward the limb and converge in the plexus region. Medial and lateral LMC motor axons show dorso-ventral guidance defects in the forelimb. In contrast, Sema3F-Npn-2 signaling guides the axons of a medial subset of LMC neurons to the ventral limb, but plays no major role in regulating their fasciculation. Thus, Sema3A-Npn-1 and Sema3F-Npn-2 signaling control distinct steps of motor axon growth and guidance during the formation of spinal motor connections.**

## Introduction

During development, axons project to their targets in a step-wise manner in response to attractive and repulsive cues that shape their trajectories (Dickson, 2002). Typically, there is a tight regulation of spatial and temporal patterns of guidance cue expression along substrates that define axon paths, as well as of the expression of corresponding neuronal receptors that signal responses to these cues. The timing of axonal growth is also constrained to ensure that growth cone extension corresponds temporally with the expression of guidance cues. In several neural systems, sets of axons have been shown to pause after arriving at specific locations, presumably permitting temporal changes in the environment or in the neuron itself that are essential for subsequent pathfinding to intermediary or final targets. Thus, regulation of the timing of axon in-growth has been observed during the establishment of thalamocortical connectivity (Ghosh and Shatz, 1993; Rakic, 1977), during the extension of olfactory sensory neurons toward the telencephalon (Gong and Shipley, 1995; Renzi et al., 2000), and during the development of sensory afferent projections to the spinal cord (Davis et al., 1989). Although the existence of waiting periods has therefore been well documented, the mechanisms that govern the timing of axon growth are still poorly understood.

The cellular mechanisms that control axonal growth have been studied intensively in the context of spinal motor neurons. In this system, motor axon projections to their targets are known to depend on a complex series of guidance events, each of which requires the temporal and spatial distribution of cues that guide axons to their peripheral muscle targets. Motor axons from defined populations of spinal motor neurons elaborate stereotypic and well-defined trajectories within the developing limb. Analysis of these guidance events provides a potential opportunity to delineate the contribution of the timing of axon outgrowth to the fidelity of target selection.

The cell bodies of motor neurons that send axons along the same peripheral trajectories reside together within the ventral spinal cord. For example, at brachial and lumbar levels of the spinal cord, motor neurons that innervate limb muscles settle in a lateral position in the spinal cord and form the lateral motor column (LMC). In contrast, the medial motor column (MMC) is found at all axial levels of the spinal cord and comprises motor neurons that project their axons to axial muscles (Hollyday, 1980; Jessell, 2000; Landmesser, 1978b). The establishment of mature motor axon projection patterns in the limb is accomplished in a stereotyped sequence of events. The axons of LMC motor neurons exit the spinal cord through the ventral roots, grow in tight fascicles along a common pathway, and converge in the plexus region at the base of the limb. Cues that mediate neuron-neuron contacts, such as cell adhesion molecules L1, NCAM, and its associated carbohydrate polysialic acid (PSA), appear to contribute to motor axon sorting and selective fasciculation at the plexus region found at the base of the limb (Tang et al., 1992, 1994). Within the plexus region, motor axons have been observed to pause before entering the limb, and during this waiting period they defasciculate and regroup into new, target-specific fascicles (Lance-Jones and Landmesser, 1981; Tosney and Landmesser, 1985b; Wang and Scott, 2000). Moreover, heterochronic limb transplantations in chicken embryos indicate that the age of the limb rather than the age of the neurons themselves dictates the time of axon in-growth, suggesting that cues in the

*Correspondence: dginty@jhmi.edu (D.D.G.); kolodkin@jhmi.edu (A.L.K.)

[4] Present address: Institute for Developmental Genetics, GSF-Research Center for Environment and Health, 85764 Neuherberg, Germany.

limb mesenchyme regulate the timing of axon invasion through their interactions with receptors on motor axons (Wang and Scott, 2000). The molecular nature of these signals is not known.

As they emerge from the plexus region, LMC axons select a dorsal or ventral trajectory within the limb mesenchyme. Motor neurons that settle in the lateral division of the LMC (LMCl) project axons to dorsally derived limb muscles, whereas medial LMC (LMCm) motor neurons send axons to ventral limb muscles (Lance-Jones and Landmesser, 1981; Landmesser, 1978a; Tosney and Landmesser, 1985a, 1985b). The initial axonal trajectory of these distinct motor neuron populations appears to be specific and accurate, implying the coordination of guidance cue expression and the timing of axonal extension (Ferguson, 1983; Hollyday, 1980; Lance-Jones and Landmesser, 1980, 1981; Landmesser, 1978a; Landmesser, 2001; Whitelaw and Hollyday, 1983). However, the consequences for motor axon pathfinding of the disruption of the precise timing of motor axon extension into the limb have not been evaluated genetically.

The spectrum of guidance cues that direct motor axons to appropriate dorsal or ventral muscle targets in the limb remains ill-defined. One interaction that has been shown to play a role in directing LMCl neurons to the dorsal limb is mediated by ephrin-A-EphA ligand-receptor signaling (Eberhart et al., 2002; Feng et al., 2000; Helmbacher et al., 2000; Kania and Jessell, 2003). Repulsive guidance mediated by interactions between the EphA4 receptor expressed in LMCl neurons and the ephrin-A ligands expressed in the ventral limb mesenchyme appears to direct LMCl axons into the dorsal limb mesenchyme (Eberhart et al., 2002, 2004; Helmbacher et al., 2000; Kania and Jessell, 2003). Nevertheless, loss- and gain-of-function experiments strongly suggest that ephrin signaling does not account for all aspects of motor axon pathfinding in the limb (Kania and Jessell, 2003; Helmbacher et al., 2000). In particular, the mechanisms that instruct the axons of LMCm motor neurons to grow into the ventral limb mesenchyme remain obscure.

Secreted semaphorin proteins have also been implicated in the control of motor axon projections (Chen et al., 2000; Giger et al., 2000; Kitsukawa et al., 1997; Taniguchi et al., 1997; Varela-Echavarria et al., 1997; Zou et al., 2000), although their precise roles have not been defined. The semaphorins are a large family of phylogenetically conserved cell surface and secreted proteins, many of which mediate repulsive guidance events during neural development. Certain secreted class 3 semaphorins, including Sema3A and Sema3F, are plausible motor axon guidance cues because they can induce the collapse of spinal motor neuron growth cones and repel motor axons in vitro (Cohen et al., 2005; Kuhn et al., 1999; Varela-Echavarria et al., 1997). Most of the class 3 secreted semaphorins signal through holoreceptor complexes that are composed of one of the four class A plexins and the obligate coreceptor neuropilin-1 (Npn-1) or neuropilin-2 (Npn-2) (Huber et al., 2003; Suto et al., 2005; Yaron et al., 2005). The neuropilins function as ligand-binding subunits, whereas plexins function as signal-transducing subunits. The diverse effects of class 3 semaphorins on axonal guidance are achieved through tightly regulated patterns of neuropilin, plexinA, and secreted semaphorin expression, together with the preferential binding of class 3 semaphorins to either Npn-1 or Npn-2 (Murakami et al., 2001; Nakamura et al., 2000). For example, Sema3A signals repulsive guidance events through interactions with Npn-1, whereas Sema3F acts through Npn-2 (Chen et al., 2000; Cheng et al., 2001; Giger et al., 2000; Kitsukawa et al., 1997; Sahay et al., 2003; Takahashi et al., 1999). Because Npn-1 and Npn-2 are expressed in developing spinal motor neurons (Chen et al., 1997; Cohen et al., 2005; He and Tessier-Lavigne, 1997; Kolodkin et al., 1997) it seems likely that Sema3-neuropilin signaling participates in motor axon guidance, although it is unclear whether these two receptors have overlapping or distinct functions.

Here, we use genetic approaches in mice and chick to show that semaphorin-neuropilin signaling regulates the timing of motor axon growth and target selection in the developing limb. Our findings indicate that Sema3A-Npn-1 signaling directs the fasciculation, timing, and fidelity of motor axon growth into the forelimb. In contrast, Sema3F-Npn-2 signaling guides the axons of a subset of LMCm neurons into the ventral forelimb through a repulsive interaction with Sema3F located in the dorsal limb mesenchyme. Thus, Sema3A-Npn-1 and Sema3F-Npn-2 signaling play distinct roles in directing spinal motor axon extension and appear to underlie aspects of the temporal coordination of motor axon outgrowth and target innervation.

## Results

### *Neuropilins* Are Differentially Expressed in Spinal Motor Neurons

Secreted semaphorins (Semas) are capable of acting as spinal motor axon repellents in vitro (Cohen et al., 2005; Kuhn et al., 1999; Varela-Echavarria et al., 1997). To determine whether Sema-neuropilin signaling is involved in regulating aspects of motor axon development in vivo, we examined *Npn-1* and *Npn-2* expression patterns in the developing mouse brachial spinal cord. We characterized the relationship between these expression patterns and specific motor neuron populations, focusing on the issue of whether *Npn-1* and *Npn-2* expression coincides with the expression of LIM homeodomain transcription factors in motor neuron columnar subsets (Tsuchida et al., 1994; Kania et al., 2000).

Analysis of neurofilament expression revealed that axons have reached the base of the forelimb, but have not yet grown into limb tissue, at embryonic day 10.5 (E10.5) (data not shown). At this stage, *Npn-1* mRNA is expressed by most, if not all, LMC neurons throughout the rostral-caudal extent of the brachial spinal cord as determined by coexpression with *Raldh2*, a marker of all LMC neurons (Figures 1C–1E). LMC motor neurons are segregated into distinct lateral and medial columnar divisions, defined by *Lim1* and *Isl1* expression, respectively (Kania et al., 2000; Sockanathan and Jessell, 1998; Tsuchida et al., 1994). *Npn-1* expression overlaps with that of *Lim1* and Isl1. *Npn-2* is not detected in *Lim1*$^+$ brachial LMCl motor neurons but is expressed in a subset of Isl1$^+$, *Raldh2*$^+$ LMCm neurons in the rostral and caudal regions of the brachial LMC (Figures 1F–1I). Taken together, these results show that *Npn-1* and

*Npn-2* are expressed in partially overlapping subpopulations of mouse brachial LMC motor neurons at a stage when motor axons make specific pathway choices.

We next analyzed the expression patterns of secreted semaphorins in relation to axon tracts in the developing mouse forelimb. To visualize the distribution of Sema3A protein, we incubated tissue sections or whole embryos with an alkaline phosphatase (AP)-tagged Npn-1 ectodomain fusion protein (Npn-1$^{ecto}$-AP). The staining patterns we observed are absent in *Sema3A*$^{-/-}$ null mutant embryos (Figure 1K), demonstrating that Npn-1$^{ecto}$-AP detects Sema3A protein in these regions. We detected robust expression of Sema3A in the developing limb bud at E10.5, when spinal nerves are in the plexus region but have not yet entered the limb (Figure 1J). Sema3A was strongly expressed at the base of the developing limb just distal to the plexus region (Figure 1L; see Figure S4A in the Supplemental Data available online). The presence of Sema3A in the limb bud at a time when motor axons have arrived at the plexus region raises the possibility that Sema3A regulates the timing of motor axon in-growth into the forelimb. At E11.5, Npn-1$^{ecto}$-AP binding revealed a high level of Sema3A expression adjacent to spinal nerve tracts within the forelimb (Figure S2C), raising the possibility that, at this later time, Sema3A regulates motor axon fasciculation. These data confirm the presence of Sema3A protein in regions that express *Sema3A* mRNA (Wright et al., 1995) and that also exhibit X-Gal staining in a *Sema3A-LacZ* knockin mutant mouse (Taniguchi et al., 1997).

To visualize the endogenous distribution of ligands for Npn-2, we probed tissue sections with an AP-tagged Npn-2 ectodomain fusion protein (Npn-2$^{ecto}$-AP) (Watanabe et al., 2004). Binding of Npn-2$^{ecto}$-AP was observed in the dorsal forelimb at E10.5 in the region in which the axons of LMC neurons bifurcate to establish dorsal and ventral limb trajectories (Figure 1L). Npn-2$^{ecto}$-AP binding was absent in *Sema3F* mutant limb tissue (Figure 1M), strongly suggesting that Npn-2$^{ecto}$-AP selectively interacts with endogenous Sema3F in this region. Sema3F has repulsive effects on Npn-2-expressing axons (Chen et al., 1997, 2000; Giger et al., 2000), raising the possibility that Sema3F protein expressed in the dorsal limb bud directs *Npn-2*-expressing LMCm axons along a ventral trajectory in the forelimb.

Because class 3 semaphorin signaling has been implicated in the regulation of neuronal cell migration (Huber et al., 2003), we examined whether loss of Npn-1, Npn-2, Sema3A, or Sema3F affects the formation of motor columns. To assess motor neuron column organization, we examined LIM homeodomain expression profiles at E12.5 in *Npn-1*$^{Sema-}$ knockin mice, where binding of all class 3 semaphorins to Npn-1 is selectively abolished while interactions with vascular endothelial growth factors (VEGFs) are maintained (Gu et al., 2003); in mice harboring a *Npn-2* null mutation (Giger et al., 2000); and in *Sema3A* (Behar et al., 1996) and *Sema3F* null mutants (Sahay et al., 2003). At E12.5 in the mouse, motor neurons have assumed their characteristic positions in the spinal cord (Arber et al., 1999). We found that in *Sema3A*, *Sema3F*, *Npn-1*$^{Sema-}$, and *Npn-2* mutants the lateral and medial LMC neuron markers, Lim1 and Isl1, respectively, are expressed in patterns characteristic of the normal settling positions for LMC neurons (Figures S1 and S1B–S1K). In addition, the number of motor neurons in the medial and lateral LMC is similar in these mutants and wild-type littermates (Figure S1A). Thus, the loss of Npn-1, Npn-2, Sema3A, or Sema3F function does not affect the specification or position of motor neuron cell bodies within the LMC.

### Precocious Extension of Motor and Sensory Projections in *Npn-1*$^{Sema-}$ and *Sema3A* Mutants

The expression of *neuropilins* in distinct populations of brachial LMC motor neurons, together with the presence of their ligands Sema3A and Sema3F in the limb bud at E10.5, prompted us to examine the formation of motor and sensory projections in the absence of semaphorin-neuropilin signaling. To label motor axons selectively, we crossed an *HB9:eGFP* transgenic mouse line (Lieberam et al., 2005; Wichterle et al., 2002) to *Npn-1*$^{Sema-}$ knockin and *Npn-2*, *Sema3F*, and *Sema3A* null mutant mice. Motor axon projections were observed in whole-mount embryo preparations by GFP expression, and sensory axons were detected by expression of neurofilament in the absence of GFP. At E10.5, when wild-type motor axon projections reach the plexus region (Figure 2A) (Tosney and Landmesser, 1985a), we observed that motor axons in both *Npn-1*$^{Sema-}$ and *Sema3A* mutants had entered the limb and made significant progress toward distal limb regions (Figures 2B and 2C, white arrowheads).

We calculated a relative extension score (RES) for motor axons by measuring the length of the longest visible motor axon extending distally from the point of tightest convergence in the plexus region and normalizing this value to the proximal-distal length of the limb (see Experimental Procedures). The RES was significantly higher in both *Npn-1*$^{Sema-}$ and *Sema3A* mutants than in wild-type littermates (Figure 2, $p < 0.01$ and $p < 0.04$, respectively, see figure legend). These observations imply that Sema3A-Npn-1 interactions normally prevent premature invasion of motor axons into the forelimb mesenchyme. In contrast, in *Npn-2* and *Sema3F* mutants, motor and sensory projections entered the limb at the same time as in wild-type embryos, extending similar distances into the forelimb at E10.5 (Figures 2D–2F). Therefore, Sema3A-Npn-1, but not Sema3F-Npn-2, signaling regulates the timing of motor and sensory axon growth into the forelimb.

### Npn-1-Sema3A Signaling Controls Fasciculation of Motor and Sensory Projections in the Forelimb Plexus

We next monitored the formation of distinct projections to the forelimb at E12.5, when motor and sensory axons have crossed the plexus region and formed individual nerve branches. In *Npn-1*$^{Sema-}$ mutants, both motor and sensory projections innervating the forelimb showed marked defasciculation and aberrant, exuberant growth when compared to wild-type embryos (Figures 3A and 3B). Nerve defasciculation was particularly pronounced in the forelimb plexus region, where axons normally converge and segregate into muscle-specific nerve bundles. In *Npn-1*$^{Sema-}$ mutants, motor axons within the plexus were defasciculated and did not converge into tight bundles (Figure 3E, arrow). We observed a similar phenotype in *Sema3A* mutant embryos: motor

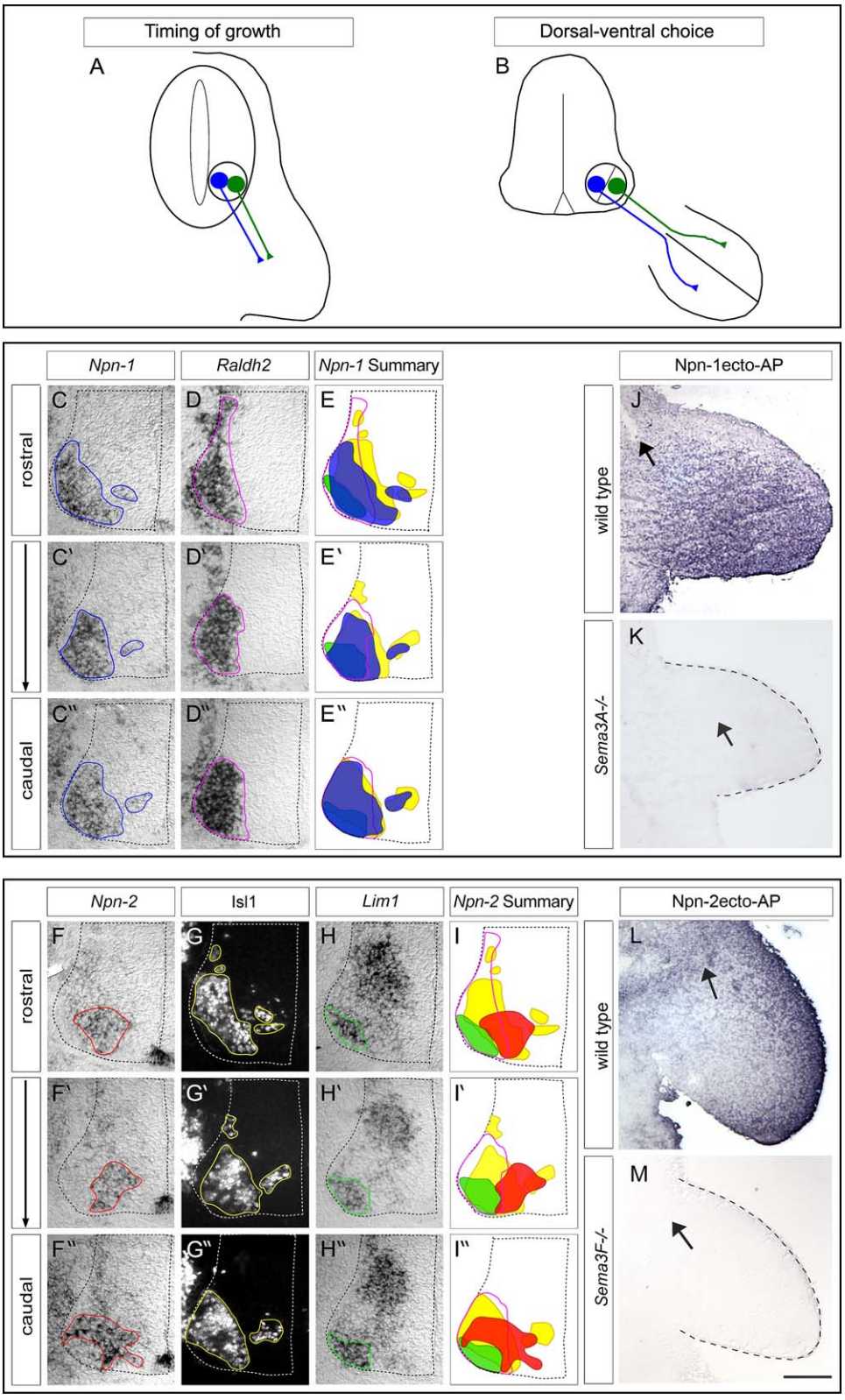


Figure 1. Expression Patterns of *Neuropilins*, *Sema3A*, and *Sema3F*

(A) Schematic drawing of motor axon extension at E10.5.

(B) Schematic drawing of motor projections at E12.5 after the establishment of the dorso-ventral choice point.

(C–I) Expression patterns of *Npn-1* and *Npn-2* are revealed on adjacent transverse sections through the mouse brachial spinal cord. Three axial levels including the forelimb LMC are shown from rostral (top row) to caudal (bottom row). The ventrolateral quadrant of the spinal cord is shown, and the spinal cord is outlined with a dashed line.

(C) *Npn-1* mRNA.

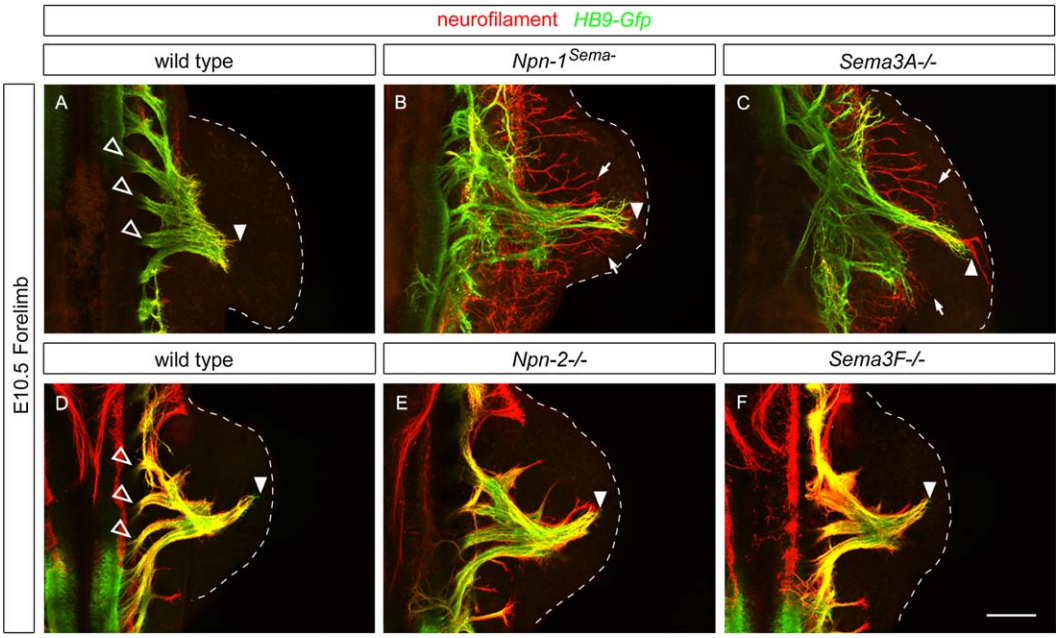


Figure 2. Premature Growth of Forelimb Motor and Sensory Projections in *Npn-1*$^{Sema-}$ and *Sema3A* Mutants

(A–C) Dorsal views of the forelimb plexus in whole-mount embryos utilizing anti-GFP (green, motor projections) and anti-neurofilament (red, motor and sensory projections) staining of E10.5 homozygous *Npn-1*$^{Sema-}$ (B), wild-type littermate (A) and *Sema3A* null (C) embryos. The relative extension score (RES, see text and Experimental Procedures) was higher in *Npn-1*$^{Sema-}$ (0.57 ± 0.07 SEM) and *Sema3A* mutants (0.92 ± 0.02 SEM) than in wild-type littermates (0.34 ± 0.02 SEM and 0.67 ± 0.08 SEM).

(D–F) Extension of motor and sensory projections is revealed in dorsal views of the forelimb plexus in E10.5 *Npn-2* (E), *Sema3F* (F) null, and wild-type littermate control embryos (D). The RES was not significantly different in either *Npn-2* (0.36 ± 0.03 SEM) or *Sema3F* mutants (0.34 ± 0.05 SEM) as compared to wild-type littermates (0.33 ± 0.04 SEM and 0.31 ± 0.04 SEM). Differences in extension of motor and sensory neurons into the limb in wild-type embryos in (A) and (D) are due to small variations in the timing of these matings, but do not influence our RES calculations because these are only performed using littermate embryos. The position of the furthest motor axon is marked with an arrowhead, spinal nerves are indicated with empty arrowheads (A and D), exuberant sensory axon growth is marked with a white arrow (B and C), and the limb buds are outlined with a dotted white line.

Scale bar, 200 μm in all panels.

and sensory axons were defasciculated and spread over a wide area at the plexus region (Figures 3C and 3F, arrow).

To quantify the degree of motor axon defasciculation in these mutants, we measured the rostrocaudal distance of motor axon spreading at three medial-to-lateral landmark positions: (1) convergence of spinal nerve branches from C4 and C5, (2) branching of the suprascapular nerve, and (3) divergence of the motor neuron branches that project caudally to the cutaneus maximus (medial anterior thoracic nerve) and latissimus dorsi (thoraco-dorsal nerve) muscles (Figure 3M; Greene, 1935). This analysis revealed a 1.5- to 2-fold expansion of the plexus region at all three reference points in both *Npn-1*$^{Sema-}$ and *Sema3A* mutants (Figure 3N). Sema3A is expressed in close proximity to growing axon tracts (Figure S2C) and is therefore likely to act through a "surround repulsion" mechanism to maintain fasciculation as axons grow toward the plexus and into the forelimb.

Is Npn-2 also involved in bundling axon projections to the forelimb? To address this issue we evaluated axonal trajectories in the forelimb of *Npn-2* (Figures 3H and 3K) and *Sema3F* (Figures 3I and 3L) mutants. No defects were observed in motor or sensory axonal fasciculation, compared to wild-type littermates (Figures 3G and 3J). Moreover, motor projections in *Npn-2* and *Sema3F* mutants converge tightly as they exit the spinal cord to form

(D) *Raldh2* mRNA.

(E) Schematic overlay of expression areas: *Npn-1* (blue), Isl1 (yellow), *Raldh2* (purple).

(F) *Npn-2* mRNA.

(G) Isl1 protein, immunohistochemistry performed on the same section as *Npn-2* in situ hybridization in (F).

(H) *Lim1* mRNA.

(I) Overlay of expression domains: *Npn-2* (red), Isl1 (yellow), *Lim1* (green), *Raldh2* (purple).

(J) Binding of Npn-1$^{ecto}$-AP to forelimb sections of E10.5 wild-type embryos reveals strong expression of Sema3A in the forelimb bud (outlined with a dashed white line). No binding was detected in *Sema3A* mutant embryonic limb buds (K). The forelimb bud is outlined with a black dashed line and the most distal extent of the spinal nerve, as determined by neurofilament staining (not shown), is indicated in each section with a black arrow.

(L) Section overlay assay with Npn-2$^{ecto}$-AP reveals the distribution of Sema3F in wild-type embryos at E10.5 in the dorsal region of the forelimb. No binding of Npn-2$^{ecto}$-AP for E10.5 forelimb sections was detected on *Sema3F* mutant tissue (M) (dashed line and arrows as in [J]).

Scale bar, 115 μm in (A)–(I) and 140 μm in (J)–(M).

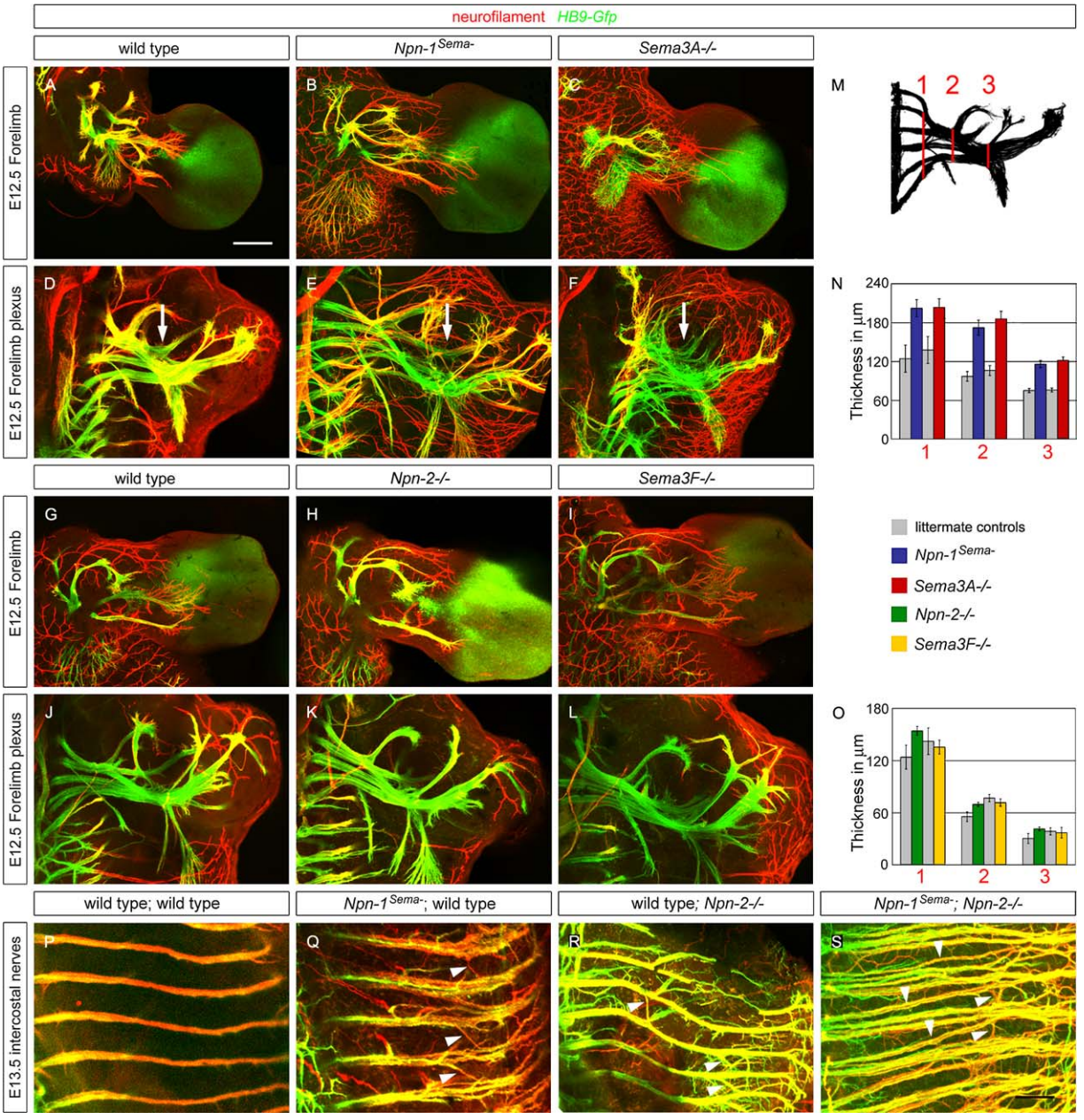


Figure 3. Defasciculation of LMC and MMC Projections in *Npn* and *semaphorin* Mutant Mice

(A–F) Whole-mount anti-GFP (green, motor axons) and anti-neurofilament (red, motor and sensory axons) staining of E12.5 homozygous *Npn-1*$^{Sema-}$ (B and E), wild-type littermate (A and D), and *Sema3A* null (C and F) embryos show defasciculated motor and sensory projections in the forelimb in the absence of Sema-A-Npn-1 signaling.

(D–F) Enlarged dorsal views of the plexus of the forelimbs shown in (A)–(C). The arrow points to the plexus region, where defasciculation of motor and sensory projections is revealed in *Npn-1*$^{Sema-}$ (E) and *Sema3A* null (F) embryos.

(G–L) Whole-mount embryo preparations at E12.5 of *Npn-2* (H and K), *Sema3F* (I-L), and wild-type littermate embryos (G and J) all show normal fasciculation of motor and projections in the forelimb.

(J–L) Enlarged dorsal views of the plexus region of the forelimbs depicted in (G)–(I).

(M–O) Quantification of motor axon convergence at the plexus. The thickness of the plexus was measured on six limbs of each genotype at the three landmark points indicated in (M).

(P–S) Detection of GFP (green, motor axons) and neurofilament (red, motor and sensory fibers) in whole-mount embryo preparations at E13.5 reveals defasciculated intercostal nerves in *Npn-1*$^{Sema-}$ (Q), *Npn-2* null (R), and *Npn-1*$^{Sema-}$*;Npn-2* double mutant embryos (S) as compared to wild-type littermate embryos (P). Arrowheads mark aberrant axon projections between intercostal nerves.

Scale bar, 300 μm in (A)–(C) and (G)–(I), 120 μm in (D)–(F) and (J)–(L), and 100 μm in (P)–(S).

the brachial plexus (Figures 3K and 3L): plexus thickness measured at the three reference points was indistinguishable in both *Npn-2* and *Sema3F* mutants and their control littermate embryos (Figure 3O). Axonal defasciculation at the forelimb plexus was not enhanced in *Npn-1*$^{Sema-}$*;Npn-2* double mutants over what we

observed in *Npn-1*$^{Sema}$ or Sema3A single mutants (data not shown), further suggesting that *Npn-2* is not involved in regulating the fasciculation of LMC axonal projections to the forelimb.

To address whether Sema3s are involved in the fasciculation of other spinal motor projections, we assessed the effect of semaphorin-neuropilin signaling on the fasciculation of thoracic intercostal nerves, which contain the axons of lateral MMC motor neurons. We found that wild-type intercostal nerves are tightly fasciculated at E13.5 (Figure 3P). In contrast, intercostal nerves are defasciculated in *Npn-1* or *Npn-2* single mutants (Figures 3Q and 3R), with many nerve braches crossing between main nerve tracts (arrowheads). This phenotype is dramatically enhanced in the *Npn-1*$^{Sema-}$*;Npn-2* double mutant, and here defasciculation of intercostal nerves was so pronounced that the main intercostal bundles no longer appear to respect somite boundaries and were spread over the entire thoracic region (Figure 3S). The major Npn-1 and Npn-2 ligands, Sema3A and Sema3F, respectively, are expressed in the caudal somite at E10.5, as revealed by Npn$^{ecto}$-AP binding to whole embryos (Figures S2A and S2B). These results suggest that in the thoracic regions, unlike the forelimb, Sema3A-Npn-1 and Sema3F-Npn-2 signaling collaborate to control the fasciculation of MMC axonal projections to intercostal muscles.

### Npn-1-Sema3A Signaling Is Required for Correct Dorso-Ventral Trajectories of LMC Axons in the Forelimb

Does the precocious entry of motor axons into the forelimb in the *Npn-1*$^{Sema-}$ and *Sema3A* mutants lead to defects in the stereotypical dorso-ventral choices made by LMC axons? Because in *Npn-1*$^{Sema-}$ and *Sema3A* mutants motor nerves are defasciculated in the plexus region, we examined whether the absence of Sema3A-Npn-1 signaling leads to pathfinding defects in the limb. We retrogradely labeled motor neuron cell bodies by injecting horseradish peroxidase (HRP) into either the ventral or dorsal forelimb muscles of E13.5 *Npn-1*$^{Sema-}$ and *Sema3A* mutant embryos and then assessed the presence of retrogradely transported HRP in the cell bodies of Lim1$^+$ LMCl motor neurons and Isl1$^+$ LMCm motor neurons. In wild-type embryos, nearly all of the HRP-labeled motor neurons that were retrogradely labeled from dorsal forelimb muscle injections expressed Lim1 but not Isl1 (97%; Figure 4B; data not shown). In contrast, significantly more dorsally labeled HRP$^+$ motor neurons expressed Isl1 in *Npn-1*$^{Sema-}$ (22%) and *Sema3A* mutant embryos (24%; Figures 4C and 4D, arrowheads) as compared to wild-type littermates. These misrouted LMCm neurons did not express Lim1 (data not shown). Following injection into the ventral muscle mass of wild-type embryos, HRP is detected primarily in Isl1$^+$ LMCm neurons, with only 2% of ventrally HRP-labeled neurons expressing Lim1 (Figure 4F, data not shown). However, in *Npn-1*$^{Sema-}$ embryos, 35% of HRP$^+$ neurons expressed Lim1 following ventral HRP injections (Figure 4G, arrowheads; data not shown). Thus, a substantial fraction of LMCl neurons embark on an inappropriate trajectory to the ventral forelimb in *Npn-1*$^{Sema-}$ mutant embryos. The low incidence of LMC motor neurons with apparent dorsal or ventral axonal misprojections in wild-type embryos is likely to be the result of tracer injection errors, because independent genetic tracing reveals that the fidelity of this dorso-ventral guidance decision is normally extremely high (Kania et al., 2000).

We asked whether loss of Sema3A, the major ligand for Npn-1, leads to projection errors in LMCl neurons by evaluating the course taken by LMCl axons in *Sema3A* mutant embryos. We found that significantly more Lim1$^+$ LMCl neurons projected axons aberrantly to the ventral forelimb (19% of HRP$^+$ neurons, Figure 4H, arrowheads) as compared to wild-type embryos (5% of HRP$^+$ neurons). EphA4 is expressed by LMCl neurons and their axons and provides an independent measure of LMCl axonal projections to the limb (Helmbacher et al., 2000; Kania and Jessell, 2003). We observed that expression of EphA4 in LMCl neurons is unchanged in the absence of Sema3A-Npn-1 signaling (data not shown). Consistent with our retrograde tracing observations, in both *Npn-1*$^{Sema-}$ and *Sema3A* mutant embryos EphA4$^+$ axons that originated from LMCl motor neurons aberrantly projected into the ventral forelimb mesenchyme (Figures 4J–4P). Quantitative immunofluorescence analysis of EphA4 expression on axonal projections in the limb at E13.5 revealed a higher level of EphA4 expression on ventral axons in *Npn-1*$^{Sema-}$ (1.3 ± 0.25 ratio of dorsal to ventral fluorescence intensity) and *Sema3A* (1.1 ± 0.01) mutant embryos, as compared to wild-type littermates (2.2 ± 0.2, for *Npn-1*$^{Sema-}$ littermates; 2.2 ± 0.2, for *Sema3A* littermates), consistent with the presence of aberrantly projecting lateral LMC axons (Figure 4M). These results show that Sema3A-Npn-1 signaling is required for the establishment of accurate medial and lateral LMC neuron projections in the forelimb.

### Npn-1 Is Required Autonomously in Neurons for Correct Dorso-Ventral Motor Axon Projections into the Forelimb

Because the dorso-ventral pathfinding choice of LMC axons is compromised in the absence of Sema3A-Npn-1 signaling, we asked whether Npn-1 expression by motor neurons is required for accurate axonal pathfinding in the forelimb. We first examined whether the *Npn-1*$^{Sema-}$ neurons of the lateral LMC that exhibit an inappropriate axonal trajectory in the forelimb indeed express *Npn-1*. To identify misrouted LMCl neurons, we injected HRP into the ventral forelimb musculature of E13.5 *Npn-1*$^{Sema-}$ embryos and assayed the distribution of HRP/Lim1 and *Npn-1* transcript because *Npn-1* is still expressed in these mutants. We found that the majority of LMCl neurons that projected aberrantly to the ventral forelimb expressed *Npn-1* (Figures 5A–5C, white arrowheads), suggesting that Npn-1 expression in motor neurons is critical for the formation of dorso-ventral axonal trajectories. We also examined whether removal of *Npn-1* from motor neurons results in aberrant limb projections. This was achieved using a conditional allele of *Npn-1* (*Npn-1*$^{C}$) (Gu et al., 2003) and an *Isl1-Cre* line (Srinivas et al., 2001). In addition to motor neurons, Isl1 is also expressed in dorsal root ganglia (DRG) sensory neurons, and so this *Isl1-Cre* line eliminates Npn-1 from both motor and DRG sensory neurons. However, analysis in the embryonic chicken suggests that sensory

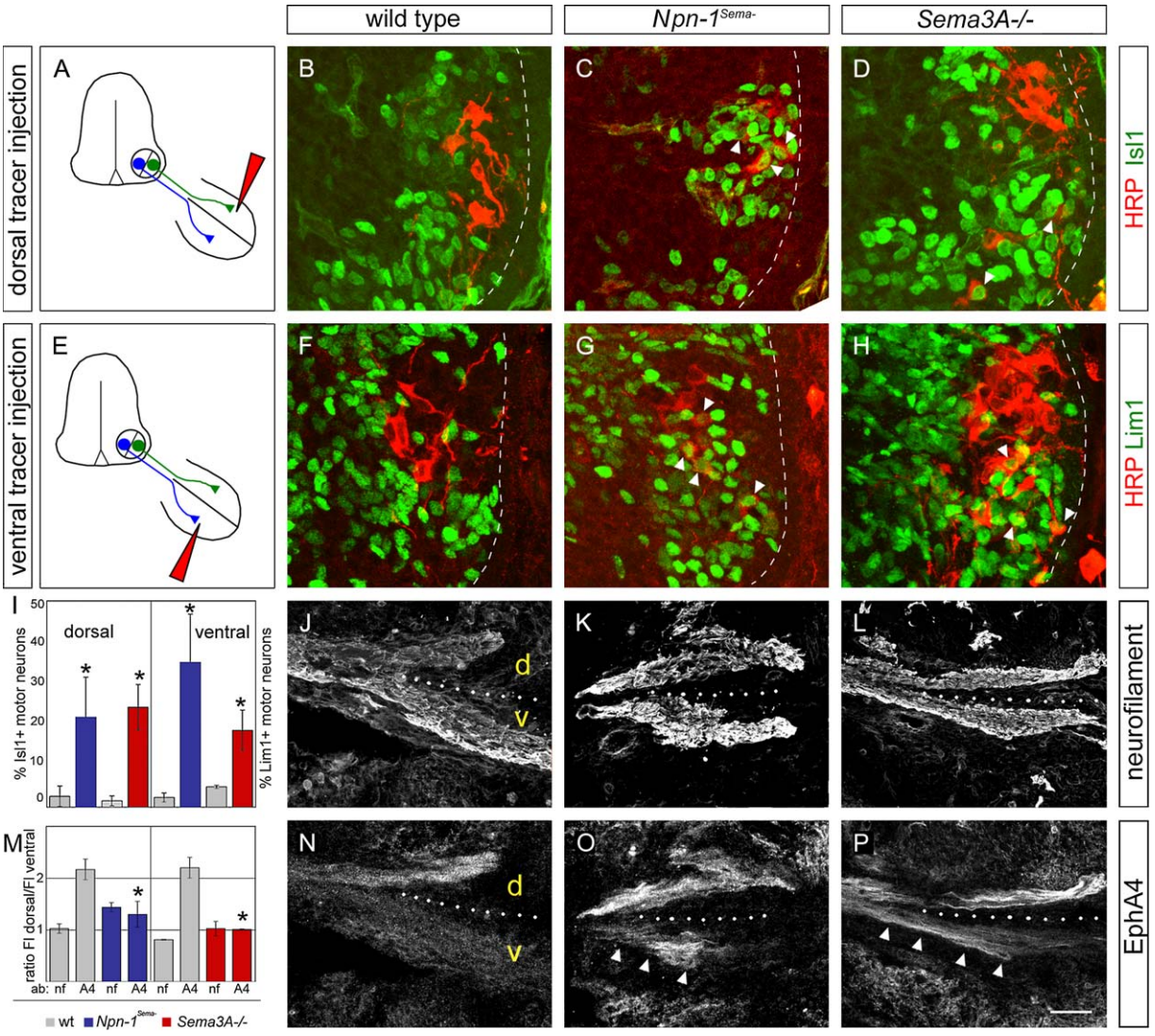


Figure 4. LMC Projections Are Misrouted in the Absence of Sema3A-Npn-1 Signaling

(A–D) Motor axon projections to the dorsal forelimb were traced using HRP retrograde labeling at E13.5. (B) In wild-type embryos, only 2.6% ± 2.5 SEM (n = 4) of $HRP^+$ (red) were also $Isl1^+$.

(C) A significant number of backfilled, $HRP^+$ motor neurons also expressed Isl1 in homozygous *Npn-1*$^{Sema-}$ mutants (21.8% ± 9.7 SEM, n = 4, $p < 0.05$) and also in *Sema3A* null embryos (D) (24.2% ± 5.5 SEM, n = 4, $p < 0.02$).

(E–H) Motor neuron projections into the ventral forelimb illuminated by HRP retrograde labeling from ventral muscles performed at E13.5.

(F) In wild-type embryos, HRP (red) is largely restricted to $Lim1^-$, medial LMC neurons, with only 2.3% (±1.1 SEM, n = 5) of $HRP^+$ neurons being $Lim1^+$.

(G) In homozygous *Npn-1*$^{Sema-}$ mutants, 35.1% (±11.7 SEM, n = 5, $p < 0.01$) of HRP-labeled LMCl neurons are also $Lim1^+$ (green). This same phenotype is also observed in *Sema3A* null embryos (D), where 18.6% (±4.9 SEM, n = 5, $p < 0.03$) of HRP-labeled neurons are also $Lim1^+$. The ventrolateral quadrant of the spinal cord is shown, and the spinal cord is outlined with a dashed white line. Misprojecting neurons are marked with arrowheads.

(I) Quantification of dorsal and ventral retrograde labeling of motor neurons. Percentage of retrogradely labeled $HRP^+$ motor neurons that are $Isl1^+$ following dorsal HRP injections and that are $Lim1^+$ following ventral HRP injections are shown.

(J–L) Anti-neurofilament and anti-EphA4 (N-P) immunostaining in E13.5 homozygous *Npn-1*$^{Sema-}$ (K and O), wild-type littermate (J and N), and *Sema3A* null (L and P) embryos. The position of the boundary between dorsal and ventral limb mesenchyme is indicated by dotted lines, and misrouted $EphA^+$ axons in *Npn-1*$^{Sema-}$ (O) and *Sema3A* null (P) embryos are marked with arrowheads.

(M) Quantification of EphA4 immunofluorescence. The immunofluorescence intensities of anti-EphA4 and anti-neurofilament staining of E13.5 ventral (v) and dorsal (d) braches were determined and the ratios of dorsal to ventral fluorescence were calculated. Higher levels of EphA4 expression were observed on ventral axons in *Npn-1*$^{Sema-}$ (1.3 ± 0.25 ratio of dorsal versus ventral fluorescence intensity) and *Sema3A* (1.1 ± 0.01) mutant embryos as compared to wild-type littermates (2.17 ± 0.2, $p < 0.03$ for *Npn-1*$^{Sema-}$ littermates and 2.2 ± 0.2, $p < 0.02$ for *Sema3A* littermates (n = 3 for mutants and their wild-type littermates).

Scale bar, 15 μm in (B)–(H) and 50 μm in (J)–(P).

axons grow into the hindlimb after motor axons (Honig et al., 1986; Landmesser and Honig, 1986; Tosney and Hageman, 1985a, 1989; Wang and Scott, 1999). Retrograde tracing from ventral forelimb muscles revealed that 35% of HRP-labeled motor neurons expressed Lim1 and therefore projected aberrantly to the ventral

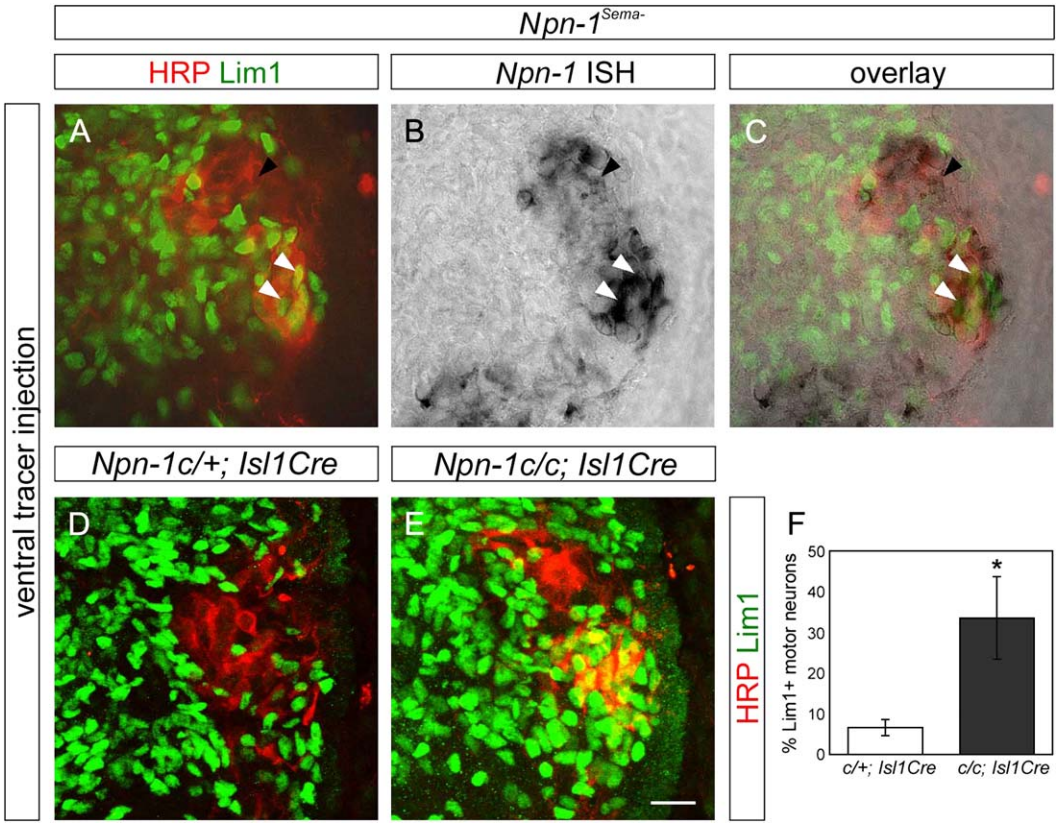


Figure 5. Cell-Autonomous Role of Npn-1 in Motor Neurons

(A) Following HRP (red) injection into the ventral forelimb of E13.5 homozygous *Npn-1*$^{Sema-}$ embryos, many HRP$^+$ motor neurons are also Lim1$^+$ (green) LMCl neurons that aberrantly project to ventral mesenchyme (white arrowheads). The correctly projecting medial LMC neurons are HRP$^+$, Lim1$^-$ (black arrowhead).

(B) *Npn-1* in situ hybridization on an adjacent section shows that misprojecting LMCl neurons in homozygous *Npn-1*$^{Sema-}$ mutants express *Npn-1*.

(C) Overlay of (A) and (B).

(D) In heterozygous *Npn-1conditional;IslCre (Npn-1 c/+;Is1lCre)* embryos following ventral HRP injections, only a small number of retrogradely labeled HRP$^+$ and Lim1$^+$ LMCl neurons are observed (5.3% ± 1.6 SEM, n = 3).

(E) Ventral HRP injections in homozygous *Npn-1 conditional;Isl1Cre (Npn-1 c/c;Isl1Cre)* at E13.5 show that 35% (±8.1 SEM, n = 3, $p < 0.01$) of HRP$^+$ motor neurons are misrouted Lim1$^+$ (green) LMCl neurons. The ventrolateral quadrant of the spinal cord is outlined with a white dashed line.

(F) Quantification of the retrograde HRP labeling and LMCl motor neuron identity.

Scale bar, 15 μm in all panels.

forelimb in mice homozygous for *Npn-1*$^C$ and heterozygous for *Isl1-Cre* (Figure 5E), as compared to 5% of Lim1$^+$ HRP-labeled motor neurons in control littermates (heterozygous for *Npn-1*$^C$ and *Isl1-Cre*, Figure 5D). These results suggest that Npn-1 is required autonomously in motor neurons to guide their axons to forelimb muscle targets.

### The Ventral Forelimb Trajectories of LMCm Axons Depend upon Sema3F-Npn-2 Signaling

The finding that *Npn-2* is selectively expressed in a subset of LMCm neurons and that Sema3F protein is found in the dorsal forelimb (Figures 1F–1I and 1L) raises the possibility that Npn-2 and Sema3F are required to direct LMCm axons along their ventral trajectory. We combined genetic loss-of-function analyses in *Sema3F* and *Npn-2* null mice with gain-of-function experiments in chick to address this issue. We first identified the cell bodies of dorsally projecting motor neurons in *Npn-2* and *Sema3F* mutant embryos and wild-type littermates by injecting HRP into the dorsal forelimb musculature at E13.5. Wild-type littermates showed a low incidence of dorsally projecting HRP$^+$, Isl1$^+$ LMCm neurons (7% and 5% of all HRP$^+$ motor neurons for *Npn-2* and *Sema3F* wild-type littermates, respectively; Figure 6B). In *Npn-2* mutants, however, a significantly higher number of HRP$^+$, Isl1$^+$ LMCm neurons projected aberrantly into the dorsal limb (37% of all HRP$^+$ motor neurons; Figure 6C, arrowheads). In *Sema3F* mutants we observed a similar guidance defect (32% HRP$^+$, Isl1$^+$ LMCm neurons; Figure 6D, arrowheads). Moreover, these misrouted Isl1$^+$ LMCm neurons lacked Lim1 expression (data not shown).

We next assessed the trajectory taken by LMCl neurons using retrograde HRP labeling of motor neurons from ventral forelimb muscles. Ventral HRP injections labeled very few Lim1$^+$ LMCl neurons in wild-type and *Npn-2* mutant embryos (9% for *Npn-2* null and 3% for wild-type littermates; Figures 6F and 6G). Further, loss of *Sema3F* did not significantly perturb the dorsal

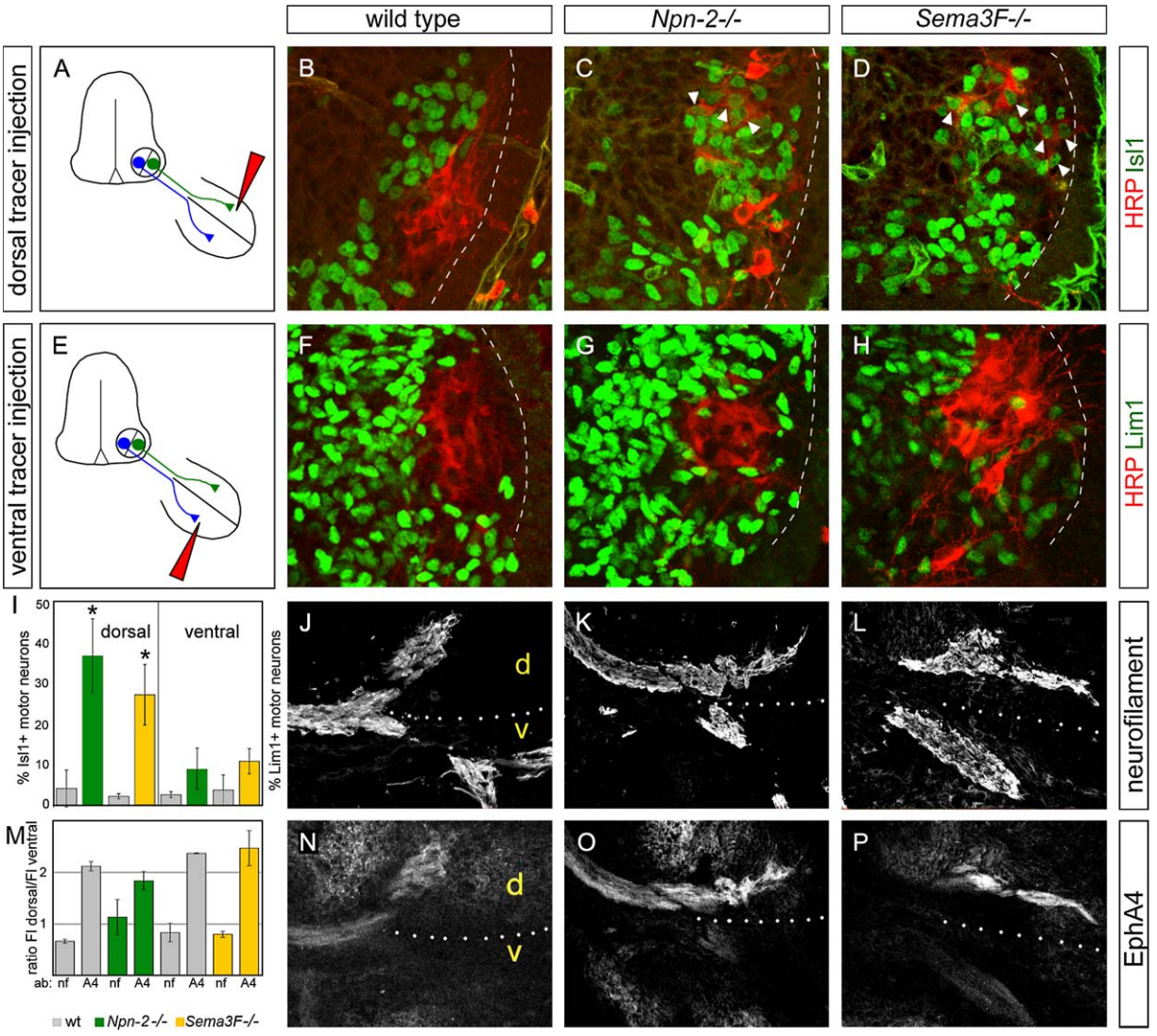


Figure 6. Misrouting of Medial LMC Neurons in *Npn-2* and *Sema3F* Mutants

(A–D) Dorsally projecting neurons are retrogradely labeled by dorsal HRP injection at E13.5. In wild-type embryos (B), $HRP^+$ neurons are mostly $Isl1^-$ (5.2% $Isl1^+$, ±5.2 SEM, n = 5). In *Npn-2* mutant embryos (C), 36.6% (±9.1 SEM) of $HRP^+$ are $Isl1^+$ medial LMCm neurons (n = 5, $p < 0.02$), and in *Sema3F* null embryos (H), 32.3% (±7.4 SEM) of $HRP^+$ neurons are also $Isl1^+$.

(E–H) HRP injection into ventral forelimb muscles at E13.5 in *Npn-2* ([G], 8.8% ± 5.2 SEM of $HRP^+$ neurons are $Lim1^+$; n = 5, p = 0.4), *Sema3F* null embryos ([H], 13.3% ± 3.1 SEM of $HRP^+$ neurons are $Lim1^+$; n = 5, p = 0.1), and wild-type littermate embryos ([F], 2.6% ± 0.7 SEM of $HRP^+$ neurons are $Lim1^+$; n = 5) reveal normal LMCl projections. The ventrolateral quadrant of the spinal cord is outlined with a dashed line.

(I) Quantification of dorsal and ventral retrograde labeling experiments. Percentages of $HRP^+$ motor neurons that are also $Isl1^+$ for dorsal injection and $Lim1^+$ for ventral injections are shown.

(J–L) Anti-neurofilament and anti-EphA4 (N-P) staining of forelimb neuronal trajectories at E13.5. The dorsal (d)-ventral (v) boundary within the forelimb is indicated with a dotted line.

(M) Quantification of the anti-EphA4 and anti-neurofilament immunostaining. Ratios of anti-EphA4 fluorescence intensities of dorsal to ventral branches are indicated.

Scale bar, 15 μm in (B)–(H) and 50 μm in (J)–(P).

trajectory taken by LMCl neurons (4% in wild-type and 14% in mutant embryos; Figure 6H; $p > 0.05$). Expression of EphA4, a marker for dorsally projecting LMCl axons, was not detected on axons in the ventral limb of *Npn-2* and *Sema3F* mutants (Figures 6J–6P). Importantly, the expression of EphA4 in LMCl neuron cell bodies was unchanged in *Npn-2* mutants (data not shown). The quantification of immunofluorescence staining for EphA4 revealed no differences in the dorsal-to-ventral ratio in *Npn-2* and *Sema3F* mutants as compared to wild-type littermates (Figure 6M). Together, these findings show that within the forelimb Sema3F-Npn-2 signaling controls the axonal trajectory of a subset of $Isl1^+$ LMCm neurons that express *Npn-2*. The repulsive ligand Sema3F is present in the dorsal limb (Figure 1C) and is likely to repel Npn-2-expressing LMCm axons and guide them into the ventral region of the limb. *Npn-2* is not expressed in LMCl neurons (Figures 1F–1I′′), and consistent with

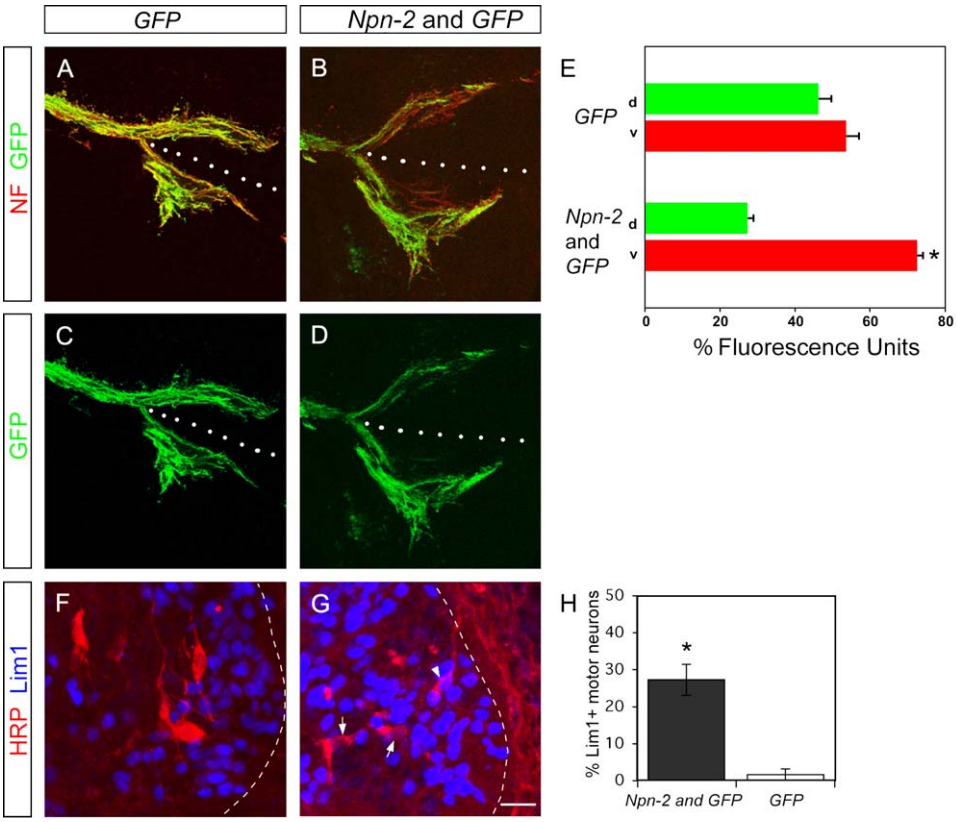


Figure 7. Overexpression of *Npn*-2 in the Chick Spinal Cord Drives Lateral LMC Axons into the Ventral Forelimb

(A–D) Anti-neurofilament (red) and anti-GFP (green) immunohistochemistry in the forelimb of stage 26 chick embryos electroporated at stage 12 with a *GFP* (n = 5, [A and B]) or *Npn-2,GFP* expression constructs (n = 7, [C and D]). The dotted line indicates the boundary between the dorsal (d) and ventral (v) forelimb.

(E) Quantification of axonal GFP immunofluorescence in forelimbs of electroporated embryos. Axonal GFP levels within the dorsal and ventral limb mesenchyme are expressed as a percentage of total limb axonal GFP immunofluorescence, $p < 0.002$.

(F and G) Retrograde tracing of ventrally projecting neurons by injecting HRP into the pectoralis muscle following electroporation of *GFP* alone (F) or *Npn-2,GFP* (G).

(H) Quantification of ventrally projecting neurons. 27.3% (±4.2 SEM, n = 8, $p < 0.02$) of $HRP^+$ (red) neurons are also $Lim1^+$ (blue, arrowhead in [G]) after injection of *Npn-2,GFP*, while only 1.6% (±1.6 SEM, n = 4) of $HRP^+$ neurons were $Lim1^+$ in *GFP*-only electroporations. $HRP^+$, $Lim1^-$ LMCm neurons that correctly project to the ventral limb are marked with arrows in (G). The ventro-lateral quadrant of the spinal cord is shown and outlined with a white dashed line.

Scale bar, 100 μm in (A)–(D) and 15 μm in (F)–(G).

this observation, disruption of Sema3F-Npn-2 signaling had no significant effect on the dorsal pathfinding of LMCl axons.

Is Npn-2 expression able to impose a ventral trajectory on LMC neurons? We addressed this issue by ectopically expressing *Npn-2* and *GFP* in brachial LMC neurons in the chick spinal cord (Figure 7; Figure S3; Kania and Jessell, 2003). In stage 23 chick spinal cord, *Npn-2* is expressed in a subset of $Isl1^+$ LMCm neurons (Figures S3D–S3G), a pattern similar to that observed in mouse. The ectopic expression of Npn-2 and GFP did not affect the expression profiles of Isl1 or Lim1, indicating that Npn-2 does not dramatically influence motor neuron development or settling patterns within the LMC in this gain-of-function paradigm (data not shown). To determine the fraction of $GFP^+$ axons that project dorsally or ventrally, we quantified axonal GFP immunofluorescence intensity in the dorsal and ventral axon branches within the forelimb (Kania and Jessell, 2003). We found that overall axonal fluorescence levels were similar, independent of whether *Npn-2* is coexpressed with *GFP* in the ventral spinal cord, suggesting that ectopic *Npn-2* expression does not affect overall LMC axonal number. Following electroporation of *GFP* alone, we observed 54% of axonal GFP fluorescence in the ventral limb and 47% in the dorsal limb (Figures 7A, 7B, and 7E). In contrast, ectopic expression of *Npn-2* and *GFP* resulted in 73% of axonal GFP fluorescence in the ventral limb and 27% in the dorsal limb ($p < 0.002$; Figures 7A–7E). Thus, ectopic expression of *Npn-2* in LMC neurons promotes the selection of a ventral axonal trajectory into the forelimb.

To determine whether *Npn-2* redirects axonal projections of LMCl neurons that ectopically express Npn-2, we injected HRP into the ventral pectoralis musculature and analyzed the status of *Lim1* expression in HRP-labeled LMC neurons. In embryos electroporated with *GFP*, only 2% of HRP-labeled neurons expressed *Lim1* (Figures 7F and 7H). Following ectopic *Npn-2* expression, however, we observed that 27% of HRP-labeled neurons expressed *Lim1* (Figure 7, arrowheads in G and H). These misrouted LMCl neurons did not express

Isl1 (data not shown). Together, these experiments suggest a role for Npn-2 in the formation of the ventral axonal trajectory of LMCm neurons in the developing limb.

## Discussion

Motor neurons project their axons to target muscles with considerable accuracy. The environment through which axons extend changes markedly during embryonic development, suggesting that the timing of axonal growth must be tightly coordinated with the temporal expression of axonal guidance cues. Neuropilins, secreted semaphorin coreceptors, are expressed in overlapping but distinct populations of spinal motor neurons, and Sema3 ligands are expressed in the developing limb. We discuss below how differential Sema3-neuropilin signaling directs specific steps in motor axon guidance that are critical for the formation of precise nerve-muscle connections (Figure 8).

### Timing of Motor Axon Ingrowth and Its Role in the Dorso-Ventral Trajectory Choice

Motor axons leave the spinal cord and converge at the plexus, a region of particular relevance to motor axon guidance in the developing vertebrate limb. Within the plexus region, motor axons segregate into nerve braches destined to innervate individual muscle groups (Tosney and Landmesser, 1985b). This process is thought to involve a tightly orchestrated series of interactions between motor axons and their extracellular environment in the limb. The spatial and temporal control of these interactions underlies the fidelity of nerve-muscle innervation patterns. We observe that Sema3A is expressed in the forelimb as motor axons arrive at the plexus region, prior to their invasion of the limb mesenchyme, and our findings reveal that motor axons grow into forelimb tissue prematurely in both *Sema3A* and *Npn-1*$^{Sema-}$ mutant mice. In the chick, motor axons pause at the plexus region prior to innervating the limb (Lance-Jones and Landmesser, 1981; Tosney and Landmesser, 1985b; Wang and Scott, 2000), although such a waiting period has not been documented in the mouse. Nevertheless, our data indicate that the precise timing of motor axon in-growth into the plexus is critical for the establishment of dorso-ventral axonal trajectories in the forelimb. Ephexin1, a guanine nucleotide exchange factor involved in Ephrin signaling, has similarly been shown to regulate the timing of motor axon growth into the chick limb (Sahin et al., 2005), suggesting that more than one signaling system contributes to the temporal regulation of motor axon extension into the limb. The strict regulation of the timing of motor axon growth at the plexus could delay axon extension into the developing limb until the appropriate distribution of motor axon guidance cues and/or their receptors is achieved, permitting motor axons to sort correctly into discrete nerve bundles. Consistent with this idea, the levels of expression of ephrinA and EphA4, a ligand-receptor pair critical for guiding LMCl motor axons to the dorsal limb, are observed to be very low 1 day prior to the normal time of motor axon ingrowth into the forelimb (A.K. and T.M.J., unpublished data). A delay of motor axon ingrowth at the plexus may therefore permit other guidance cues or their receptors to be expressed in patterns necessary for sorting of axons into muscle-specific nerve branches.

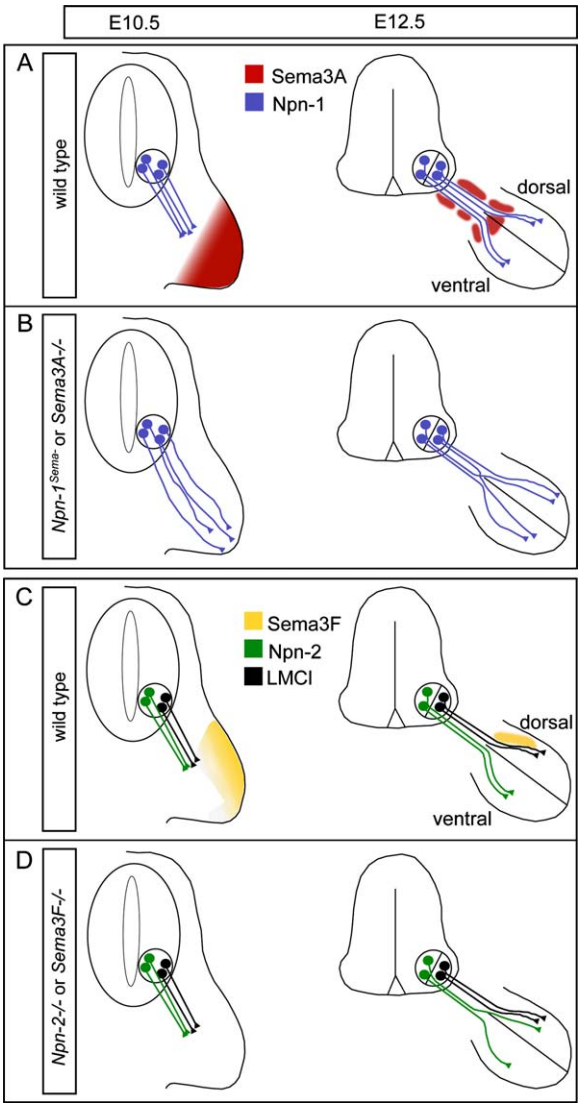


Figure 8. Model for Semaphorin-Neuropilin Signaling in LMC Axon Guidance

(A) Summary diagram of Sema3A and Npn-1 expression patterns in LMC motor neurons and limb mesenchyme at E10.5 and E12.5.

(B) In *Npn-1*$^{Sema-}$ or *Sema3A* mutant embryos, LMCm and LMCl projections enter the limb mesenchyme prematurely and are defasciculated (E10.5). The dorso-ventral choice of both LMCl and LMCm axons is disrupted.

(C) Summary diagram of Sema3F and Npn-2 expression patterns in LMCm motor neurons and forelimb mesenchyme at E10.5 and E12.5.

(D) In the absence of Npn-1 or Sema3F, motor axons enter the limb mesenchyme at the correct developmental time point and show no obvious defasciculation at E10.5. However, the absence of repulsive interactions between Npn-2-expressing LMCm neurons and Sema3F in the dorsal limb leads to an aberrant dorso-ventral choice by LMCm neurons.

### Regulation of Motor Axon Fasciculation and Subsequent Effects on Dorso-Ventral Trajectory Choice in the Limb

What role does motor axon fasciculation play in the establishment of dorso-ventral motor axon trajectories in

the limb? We find that the decrease in fasciculation of LMC axons that results from perturbation of Sema3A-Npn-1 signaling has a dramatic effect on the subsequent trajectory of these axons. In the absence of Sema3A-Npn-1 signaling, the convergence and divergence of motor axons in the plexus is disturbed. The pattern of expression of Sema3A along brachial spinal nerves and within the forelimb suggests that Sema3A has a crucial role in promoting motor axon fasciculation through a surround repulsion mechanism (Huber et al., 2003; Tessier-Lavigne and Goodman, 1996; Wright et al., 1995). Nevertheless, despite the defasciculation of motor and sensory projections in the absence of Sema3A-Npn-1 signaling, individual nerve braches that emanate distal to the plexus are still recognizable in their correct positions, implying that additional cues contribute to establishment of muscle-specific nerve trajectories. Indeed, removal of NCAM polysialic acid (PSA) in the plexus region leads to dorso-ventral axonal projection errors within the chick hindlimb (Hanson and Landmesser, 2004; Tang et al., 1992; Landmesser et al., 1988, 1990). One possible explanation for the targeting defects we observe in the absence of Sema3A-Npn-1 signaling is that defasciculation of motor nerves impairs the segregation of motor axons originating from the same motor pool. Type II cadherins and class 3 semaphorins are expressed in motor pool-specific patterns (Cohen et al., 2005; Price et al., 2002) and could be involved in the precise sorting of motor axons as they grow through the plexus region.

Although Npn-1 and Npn-2 are expressed in subsets of brachial LMC neurons, they appear to make different contributions to the fasciculation of spinal nerve projections to the limb. We observe that Sema3F-Npn-2 signaling has no major role in controlling the fasciculation of LMC projections to the forelimb. However, MMCl motor axons, which coexpress *Npn-1* and *Npn-2*, show additive defects in their projections to the intercostal muscles in *Npn-1*$^{Sema-}$*;Npn-2* double mutants. Thus, different subsets of motor neurons exhibit distinct requirements for the two neuropilin receptors.

### Npn-2 Controls Dorso-Ventral LMCm Motor Axon Trajectory Choice within the Forelimb

EphrinA-EphA4 signaling contributes to the establishment of the LMCl motor axonal trajectory to the dorsal hindlimb (Eberhart et al., 2002; Helmbacher et al., 2000; Kania and Jessell, 2003), but the mechanisms that establish the ventral axonal trajectory of LMCm neurons within the limb have remained elusive. We find that Sema3F-Npn-2 signaling plays a critical role in guiding LMCm axons into the mouse ventral forelimb. Expression of *Npn-2* in a large subset of LMCm neurons helps to direct dorso-ventral pathway selection by these motor neurons. One plausible basis for regulation of the trajectory of LMCm axons by Npn2 is through its interactions with Sema3F. Sema3F is the primary Npn-2 ligand in several projection systems (Chen et al., 2000; Giger et al., 2000; Sahay et al., 2003), and we observe that the errors made by LMCm axons in *Npn-2* mutant embryos are similar to those in *Sema3F* mutant embryos. We suggest that the expression of Sema3F in the dorsal forelimb mesenchyme normally helps to direct the ventral trajectory of wild-type LMCm axons. The evidence for repulsive signaling between dorsally expressed Sema3F in the developing limb and the axons of Npn-2-expressing LMCm neurons underscores the importance of repulsive guidance in the establishment of dorso-ventral axonal trajectories in the limb. Our analysis has focused on semaphorin-neuropilin signaling events controlling projections within the forelimb; however, it is likely that similar ligand-receptor signals coordinate dorsal and ventral axonal trajectories in both limbs. Future studies will be needed to determine the respective contributions and interactions of ephrin and semaphorin signaling in guiding motor axons at their dorso-ventral choice point in the limb.

After an initial dorso-ventral guidance decision at the plexus, motor axons diverge from main nerve trunks and project within muscle nerves toward their targets (Tosney and Landmesser, 1985a). These muscle-specific projection patterns are reflected in the spinal cord because motor neurons that project to the same peripheral targets are grouped into discrete motor pools (Haase et al., 2002; Helmbacher et al., 2003; Landmesser, 1978b; Livet et al., 2002; Price et al., 2002). The neuropilin receptors and their class 3 semaphorin ligands have been observed to be expressed in a combinatorial manner in distinct motor pools at later stages (Cohen et al., 2005), suggesting that secreted semaphorin-neuropilin signaling could also play a role in motor axon projections to specific target muscles.

The formation of complex neuronal circuits during development relies on precise responses to selectively distributed axon guidance cues. Our findings reveal that the restricted pattern of *Npn-2* expression in motor neurons contributes to the dorso-ventral choice of a subset of LMCm axons, whereas the broader expression of *Npn-1* in most LMC neurons regulates the timing of motor axon extension into the limb. Thus, we conclude that Npn-1 and Npn-2 serve distinct roles in establishing motor axon trajectories. Future genetic analyses should permit an evaluation of the degree to which the timing of axon growth and the degree of axon fasciculation influence the specificity of target selection during motor innervation. Since many populations of adult neurons, including spinal motor neurons, express secreted semaphorin receptors and are capable of responding to these repellents, the cellular and molecular mechanisms that operate during development may provide insight into the constraints on nerve regeneration following spinal injuries.

## Experimental Procedures

### Mouse Embryo Preparation

The genotype of mouse embryos was determined as described for *Npn-1*$^{sema-}$ and *Npn-1*$^{C}$ (Gu et al., 2003), *Nnp-2* (Giger et al., 2000), *Sema3A* (kind gift of Dr Behar; Behar et al., 1996), *Sema3F* (Sahay et al., 2003), *Gfp-HB9* (Wichterle et al., 2002), and *Isl1-Cre* (Srinivas et al., 2001).

### Immunohistochemistry and In Situ Hybridization

Protocols for immunohistochemistry and in situ hybridization have been described previously. For details, see the Supplemental Data online.

### Npn$^{ecto}$-AP Fusion Protein Binding

Npn$^{ecto}$-AP fusion protein binding to tissue sections and whole embryos was performed as described (Feiner et al., 1997; Watanabe

et al., 2004). Chick Npn-2$^{ecto}$-AP was a kind gift of Y. Watanabe (Watanabe et al., 2004). For details on fusion proteins, see the Supplemental Data.

### Quantification of EphA4 Axonal Levels

To quantitate axonal projections, cryostat transverse forelimb sections at E12.5 were coincubated with rabbit anti-EphA4 and mouse anti-neurofilament antibodies and Alexa488- and Alexa546-conjugated secondary antibodies (Molecular Probes). The area of highest fiber density was determined by measuring the pixel intensity of anti-neurofilament immunofluorescence in a predefined window using NIH image software. Then, the density of EphA4$^+$ fibers was quantified by measuring the pixel intensity in the green channel in the same window. The ratio of protein expression on dorsal versus ventral branches in the forelimb was calculated, and readings were performed on three embryos for each genotype.

### Retrograde Labeling of Motor Neurons

For retrograde labeling of motor neurons, 20% HRP (Sigma) and 1% lysolecithin (Sigma) in PBS were injected into several dorsal or several ventral forelimb muscles of E13.5 embryos, and preparations were incubated for 5 hr in aerated D-MEM/F12 medium (Gibco) prior to fixation in 4% PFA in PBS and immunocytochemical detection of HRP (Kania et al., 2000). Sections were triple stained with antibodies against HRP (for cytoplasmic localization), Lim1, and Isl1 (both for nuclear localization). To ensure selective dorsal or ventral labeling, sections of the injected forelimb were inspected and backfilled motor axons were evaluated; for dorsal injections, only embryos that showed no labeled axons projecting ventrally, and for ventral injections, only embryos that showed no labeled axons projecting dorsally were included in our analyses. To quantitate dorsally misprojecting neurons, backfilled HRP$^+$ neurons were counted, and the percentage of aberrantly projecting Isl1$^+$, Lim1$^-$ neurons was calculated. To quantitate the percentage of neurons that aberrantly project to the ventral forelimb, HRP$^+$ neurons were counted, and the percentage of aberrantly projecting Lim1$^+$, Isl1$^-$ neurons was calculated. The injections and quantitations were done blinded to the genotypes of the embryos.

### In Ovo Electroporation

Chick eggs were incubated and staged (Hamburger and Hamilton, 1951). In ovo electroporation of expression constructs was performed as described (Kania and Jessell, 2003). The chick *Npn-2* plasmid was a kind gift of Y. Watanabe (Watanabe et al., 2004). We used a 10-fold excess of a *Npn-2* expression construct compared to the *GFP* expression construct to ensure that all GFP$^+$ axons are likely to also express *Npn-2*, and we typically achieved ~30% electroporation of LMC neurons.

### Quantification of GFP-Labeled Axonal Projections

The quantification of motor axon projections using expression of GFP was performed as described previously (Kania and Jessell, 2003).

### Supplemental Data

The Supplemental Data for this article can be found online at http://www.neuron.org/cgi/content/full/48/6/949/DC1/.

### Acknowledgments

We thank C. Broesamle and S. Sockanathan for helpful comments on the manuscript. This work was supported by the Swiss National Science Foundation (A.B.H.), the Christopher Reeve Paralysis Foundation (A.B.H. and C.G.), the Packard Center for ALS Research at Johns Hopkins (A.L.K. and D.D.G.), and the NIH (A.L.K., D.D.G., T.M.J., and T.T.). A.K. was a Research Associate and A.L.K., D.D.G., and T.M.J. are Investigators of the Howard Hughes Medical Institute.

Received: September 20, 2005
Revised: October 25, 2005
Accepted: December 1, 2005
Published: December 21, 2005

### References

Arber, S., Han, B., Mendelsohn, M., Smith, M., Jessell, T.M., and Sockanathan, S. (1999). Requirement for the Homeobox gene Hb9 in the consolidation of motor neuron identity. Neuron *23*, 659–674.

Behar, O., Golden, J.A., Mashimo, H., Schoen, F.J., and Fishman, M.C. (1996). Semaphorin III is needed for normal patterning and growth of nerves, bones, and heart. Nature *383*, 525–528.

Chen, H., Chedotal, A., He, Z., Goodman, C.S., and Tessier-Lavigne, M. (1997). Neuropilin-2, a novel member of the neuropilin family, is a high affinity receptor for the semaphorins Sema I and Sema IV but not Sema III. Neuron *19*, 547–559.

Chen, H., Bagri, A., Zupicich, J.A., Zou, Y., Stoeckli, E., Pleasure, S.J., Lowenstein, D.H., Skarnes, W.C., Chedotal, A., and Tessier-Lavigne, M. (2000). Neuropilin-2 regulates the development of selective cranial and sensory nerves and hippocampal mossy fiber projections. Neuron *25*, 43–56.

Cheng, H.J., Bagri, A., Yaron, A., Stein, E., Pleasure, S.J., and Tessier-Lavigne, M. (2001). Plexin-A3 mediates semaphorin signaling and regulates the development of hippocampal axonal projections. Neuron *32*, 249–263.

Cohen, S., Funkelstein, L., Livet, J., Rougon, G., Henderson, C.E., Castellani, V., and Mann, F. (2005). A semaphorin code defines subpopulations of spinal motor neurons during mouse development. Eur. J. Neurosci. *21*, 1767–1776.

Davis, B.M., Frank, E., Johnson, F.A., and Scott, S.A. (1989). Development of central projections of lumbosacral sensory neurons in the chick. J. Comp. Neurol. *279*, 556–566.

Dickson, B.J. (2002). Molecular Mechanisms of Axon Guidance. Science *298*, 1959–1963.

Eberhart, J., Swartz, M.E., Koblar, S.A., Pasquale, E.B., and Krull, C.E. (2002). EphA4 constitutes a population-specific guidance cue for motor neurons. Dev. Biol. *247*, 89–101.

Eberhart, J., Barr, J., O'Connell, S., Flagg, A., Swartz, M.E., Cramer, K.S., Tosney, K.W., Pasquale, E.B., and Krull, C.E. (2004). Ephrin-A5 exerts positive or inhibitory effects on distinct subsets of EphA4-positive motor neurons. J. Neurosci. *24*, 1070–1078.

Feiner, L., Koppel, A.M., Kobayashi, H., and Raper, J.A. (1997). Secreted chick semaphorins bind recombinant neuropilin with similar affinities but bind different subsets of neurons in situ. Neuron *19*, 539–545.

Feng, G., Laskowski, M.B., Feldheim, D.A., Wang, H., Lewis, R., Frisen, J., Flanagan, J.G., and Sanes, J.R. (2000). Roles for ephrins in positionally selective synaptogenesis between motor neurons and muscle fibers. Neuron *25*, 295–306.

Ferguson, B.A. (1983). Development of motor innervation of the chick following dorsal-ventral limb bud rotations. J. Neurosci. *3*, 1760–1762.

Ghosh, A., and Shatz, C.J. (1993). A role for subplate neurons in the patterning of connections from thalamus to neocortex. Development *117*, 1031–1047.

Giger, R.J., Cloutier, J.F., Sahay, A., Prinjha, R.K., Levengood, D.V., Moore, S.E., Pickering, S., Simmons, D., Rastan, S., Walsh, F.S., et al. (2000). Neuropilin-2 is required in vivo for selective axon guidance responses to secreted semaphorins. Neuron *25*, 29–41.

Gong, Q., and Shipley, M.T. (1995). Evidence that pioneer olfactory axons regulate telencephalon cell cycle kinetics to induce the formation of the olfactory bulb. Neuron *14*, 91–101.

Greene, E.C. (1935). The Anatomy of the Rat, *Volume XXVII* (New York: Hafner Press).

Gu, C., Rodriguez, E.R., Reimert, D.V., Shu, T., Fritzsch, B., Richards, L.J., Kolodkin, A.L., and Ginty, D.D. (2003). Neuropilin-1 conveys semaphorin and VEGF signaling during neural and cardiovascular development. Dev. Cell *5*, 45–57.

Haase, G., Dessaud, E., Garces, A., de Bovis, B., Birling, M., Filippi, P., Schmalbruch, H., Arber, S., and deLapeyriere, O. (2002). GDNF acts through PEA3 to regulate cell body positioning and muscle innervation of specific motor neuron pools. Neuron *35*, 893–905.

Hamburger, V., and Hamilton, H.L. (1951). A series of normal stages in the development of the chick embryo. J. Morphol. *88*, 49–92.

Hanson, M.G., and Landmesser, L.T. (2004). Normal patterns of spontaneous activity are required for correct motor axon guidance and the expression of specific guidance molecules. Neuron *43*, 687–701.

He, S., and Tessier-Lavigne, M. (1997). Molecular basis of axonal chemorepulsion: Neuropilin is a semaphorin/collapsin receptor. Cell *90*, 739–751.

Helmbacher, F., Schneider-Maunoury, S., Topilko, P., Tiret, L., and Charnay, P. (2000). Targeting of the EphA4 tyrosine kinase receptor affects dorsal/ventral pathfinding of limb motor axons. Development *127*, 3313–3324.

Helmbacher, F., Dessaud, E., Arber, S., deLapeyriere, O., Henderson, C.E., Klein, R., and Maina, F. (2003). Met signaling is required for recruitment of motor neurons to PEA3-positive motor pools. Neuron *39*, 767–777.

Hollyday, M. (1980). Motoneuron histogenesis and the development of limb innervation. Curr. Top. Dev. Biol. *15*, 181–215.

Honig, M.G., Lance-Jones, C., and Landmesser, L. (1986). The development of sensory projection patterns in embryonic chick hindlimb under experimental conditions. Dev. Biol. *118*, 532–548.

Huber, A.B., Kolodkin, A.L., Ginty, D.D., and Cloutier, J.F. (2003). Signaling at the growth cone: Ligand-receptor complexes and the control of axon growth and guidance. Annu. Rev. Neurosci. *26*, 509–563.

Jessell, T.M. (2000). Neuronal specification in the spinal cord: inductive signals and transcriptional codes. Nat. Rev. Genet. *1*, 20–29.

Kania, A., and Jessell, T.M. (2003). Topographic motor projections in the limb imposed by LIM homeodomain protein regulation of ephrin-A:EphA interactions. Neuron *38*, 581–596.

Kania, A., Johnson, R.L., and Jessell, T.M. (2000). Coordinate roles for LIM homeobox genes in directing the dorsoventral trajectory of motor axons in the vertebrate limb. Cell *102*, 161–173.

Kitsukawa, T., Shimizu, M., Sanbo, M., Hirata, T., Taniguchi, M., Bekku, Y., Yagi, T., and Fujisawa, H. (1997). Neuropilin-semaphorin III/D-mediated chemorepulsive signals play a crucial role in peripheral nerve projection in mice. Neuron *19*, 995–1005.

Kolodkin, A.L., Levengood, D.V., Rowe, E.G., Tai, Y.T., Giger, R.J., and Ginty, D.D. (1997). Neuropilin is a semaphorin III receptor. Cell *90*, 753–762.

Kuhn, T.B., Brown, M.D., and Bamburg, J.R. (1999). Rac1-dependent actin filament organization in growth cones is necessary for beta1-integrin-mediated advance but not for growth on poly-D-lysine. J. Neurobiol. *37*, 524–540.

Lance-Jones, C., and Landmesser, L. (1980). Motoneuron projection patterns in the chick hindlimb following early partial reversals of the spinal cord. J. Physiol. *302*, 581–602.

Lance-Jones, C., and Landmesser, L. (1981). Pathway selection by chick lumbosacral motoneurons during normal development. Proc. R Soc. Lond. B Biol. Sci. *214*, 1–18.

Landmesser, L. (1978a). The development of motor projection patterns in the chick hind limb. J. Physiol. *284*, 391–414.

Landmesser, L. (1978b). The distribution of motoneurons supplying chick hind limb muscles. J. Physiol. *284*, 371–414.

Landmesser, L. (2001). The acquisition of motoneuron subtype identity and motor circuit formation. Int. J. Dev. Neurosci. *19*, 175–182.

Landmesser, L., and Honig, M.G. (1986). Altered sensory projections in the chick hindlimb following the early removal of motoneurons. Dev. Biol. *118*, 511–531.

Landmesser, L., Dahm, L., Schultz, K., and Rutishauser, U. (1988). Distinct roles for adhesion molecules during innervation of embryonic chick muscle. Dev. Biol. *119*, 645–670.

Landmesser, L., Dahm, L., Tang, J., and Rutishauser, U. (1990). Polysialic acid as a regulator of intramuscular nerve branching during embryonic development. Neuron *4*, 655–667.

Lieberam, I., Agalliu, D., Nagasawa, T., Ericson, J., and Jessell, T.M. (2005). A Cxcl12-CXCR4 chemokine signaling pathway defines the initial trajectory of Mammalian motor axons. Neuron *47*, 667–679.

Livet, J., Sigrist, M., Stroebel, S., De Paola, V., Price, S.R., Henderson, C.E., Jessell, T.M., and Arber, S. (2002). ETS gene Pea3 controls the central position and terminal arborization of specific motor neuron pools. Neuron *35*, 877–892.

Murakami, Y., Suto, F., Shimizu, M., Shinoda, T., Kameyama, T., and Fujisawa, H. (2001). Differential expression of plexin-A subfamily members in the mouse nervous system. Dev. Dyn. *220*, 246–258.

Nakamura, F., Kalb, R.G., and Strittmatter, S.M. (2000). Molecular basis of semaphorin-mediated axon guidance. J. Neurobiol. *44*, 219–229.

Price, S.R., De Marco Garcia, N.V., Ranscht, B., and Jessell, T.M. (2002). Regulation of motor neuron pool sorting by differential expression of type II cadherins. Cell *109*, 205–216.

Rakic, P. (1977). Prenatal development of the visual system in Rhesus monkey. Proc. R. Soc. Lond. B. Biol. Sci. *278*, 245–260.

Renzi, M.J., Wexler, T.L., and Raper, J.A. (2000). Olfactory sensory axons expressing a dominant-negative semaphorin receptor enter the CNS early and overshoot their target. Neuron *28*, 437–447.

Sahay, A., Molliver, M.E., Ginty, D.D., and Kolodkin, A.L. (2003). Semaphorin 3F is critical for development of limbic system circuitry and is required in neurons for selective CNS axon guidance events. J. Neurosci. *23*, 6671–6680.

Sahin, M., Greer, P.L., Lion, M.Z., Poucher, H., Eberhart, J., Schmidt, S., Wright, T.M., Shamah, S.M., O'Connell, S., Cowan, C.W., et al. (2005). Eph-dependent tyrosine phosphorylation of ephexin1 modulates growth cone collapse. Neuron *46*, 191–204.

Sockanathan, S., and Jessell, T.M. (1998). Motor neuron-derived retinoid signaling specifies the subtype identity of spinal motor neurons. Cell *94*, 503–514.

Srinivas, S., Watanabe, T., Lin, C.S., William, C.M., Tanabe, Y., Jessell, T.M., and Costantini, F. (2001). Cre reporter strains produced by targeted insertion of EYFP and ECFP into the ROSA26 locus. BMC Dev. Biol. *1*, 4.

Suto, F., Ito, K., Uemura, M., Shimizu, M., Shinkawa, Y., Sanbo, M., Shinoda, T., Tsuboi, M., Takashima, S., Yagi, T., and Fujisawa, H. (2005). Plexin-a4 mediates axon-repulsive activities of both secreted and transmembrane semaphorins and plays roles in nerve fiber guidance. J. Neurosci. *25*, 3628–3637.

Takahashi, T., Fournier, A., Nakamura, F., Wang, L.H., Murakami, Y., Kalb, R.G., Fujisawa, H., and Strittmatter, S.M. (1999). Plexin-neuropilin-1 complexes form functional semaphorin-3A receptors. Cell *99*, 59–69.

Tang, J., Landmesser, L., and Rutishauser, U. (1992). Polysialic acid influences specific pathfinding by avian motoneurons. Neuron *8*, 1031–1044.

Tang, J., Rutishauser, U., and Landmesser, L. (1994). Polysialic acid regulates growth cone behavior during sorting of motor axons in the plexus region. Neuron *13*, 405–414.

Taniguchi, M., Yuasa, S., Fujisawa, H., Naruse, I., Saga, S., Mishina, M., and Yagi, T. (1997). Disruption of semaphorin *III/D* gene causes severe abnormality in peripheral nerve projection. Neuron *19*, 519–530.

Tessier-Lavigne, M., and Goodman, C.S. (1996). The molecular biology of axon guidance. Science *274*, 1123–1133.

Tosney, K.W., and Landmesser, L. (1985a). Development of the major pathways for neurite outgrowth in the chick hindlimb. Dev. Biol. *109*, 193–214.

Tosney, K.W., and Landmesser, L. (1985b). Growth cone morphology and trajectory in the lumbosacral region of the chick embryo. J. Neurosci. *5*, 2345–2358.

Tosney, K.W., and Hageman, M.S. (1989). Different subsets of axonal guidance cues are essential for sensory neurite outgrowth to cutaneous and muscle targets in the dorsal ramus of the embryonic chick. J. Exp. Zool. *251*, 232–244.

Tsuchida, T., Ensini, M., Morton, S.B., Baldassare, M., Edlund, T., Jessell, T.M., and Pfaff, S.L. (1994). Topographic organization of embryonic motor neurons defined by expression of LIM homeobox genes. Cell *79*, 957–970.

Varela-Echavarria, A., Tucker, A., Puschel, A.W., and Guthrie, S. (1997). Motor axon subpopulations respond differentially to the chemorepellents netrin-1 and semaphorin D. Neuron *18*, 193–207.

Wang, G., and Scott, S.A. (1999). Independent development of sensory and motor innervation patterns in embryonic chick hindlimb. Dev. Biol. *208*, 324–336.

Wang, G., and Scott, S.A. (2000). The "waiting period" of sensory and motor axons in early chick hindlimb: its role in axon pathfinding and neuronal maturation. J. Neurosci. *20*, 5358–5366.

Watanabe, Y., Toyoda, R., and Nakamura, H. (2004). Navigation of trochlear motor axons along the midbrain-hindbrain boundary by neuropilin 2. Development *131*, 681–692.

Whitelaw, V., and Hollyday, M. (1983). Neuroal pathway constraints in the motor innervation of the chick hindlimb following dorsoventral rotations of distal limb segments. J. Neurosci. *3*, 1226–1233.

Wichterle, H., Lieberam, I., Porter, J.A., and Jessell, T.M. (2002). Directed differentiation of embryonic stem cells into motor neurons. Cell *1100*, 385–397.

Wright, D.E., White, F.A., Gerfen, R.W., Silos-Santiago, I., and Snider, W.D. (1995). The guidance molecule semaphorin III is expressed in regions of spinal cord and periphery avoided by growing sensory axons. J. Comp. Neurol. *361*, 321–333.

Yaron, A., Huang, P.H., Cheng, H.J., and Tessier-Lavigne, M. (2005). Differential requirement for Plexin-A3 and -A4 in mediating responses of sensory and sympathetic neurons to distinct class 3 Semaphorins. Neuron *45*, 513–523.

Zou, Y., Stoeckli, E., Chen, H., and Tessier-Lavigne, M. (2000). Squeezing axons out of the gray matter: a role for slit and semaphorin proteins from midline and ventral spinal cord. Cell *102*, 363–375.